OPEN ACCESS

TRANSLATIONAL SCIENCE

Deciphering the role of cDC2s in Sjögren's syndrome: transcriptomic profile links altered antigen processes with IFN signature and autoimmunity

Ana P Lopes ,[1,2] Maarten R Hillen,[1,2] Anneline C Hinrichs,[1,2] Sofie LM Blokland,[1,2] Cornelis PJ Bekker,[1,2] Aridaman Pandit ,[1,2] Aike A Kruize,[1] Timothy RDJ Radstake,[1,2] Joel A van Roon[1,2]

Handling editor Josef S Smolen

► Additional supplemental material is published online only. To view, please visit the journal online (http://dx.doi.org/10.1136/ard-2022-222728).

[1]Department of Rheumatology & Clinical Immunology, University Medical Center Utrecht, Utrecht University, Utrecht, The Netherlands
[2]Center for Translational Immunology, University Medical Center Utrecht, Utrecht University, Utrecht, The Netherlands

Correspondence to
Dr Joel A van Roon, Rheumatology & Clinical Immunology/Lab Translational Immunology, UMC Utrecht, Utrecht, 3584 CX, The Netherlands; j.vanroon@umcutrecht.nl

Received 29 April 2022
Accepted 25 August 2022
Published Online First 28 September 2022

To cite: Lopes AP, Hillen MR, Hinrichs AC, *et al*. *Ann Rheum Dis* 2023;**82**:374–383.

ABSTRACT

Objective Type 2 conventional dendritic cells (cDC2s) are key orchestrators of inflammatory responses, linking innate and adaptative immunity. Here we explored the regulation of immunological pathways in cDC2s from patients with primary Sjögren's syndrome (pSS).

Methods RNA sequencing of circulating cDC2s from patients with pSS, patients with non-Sjögren's sicca and healthy controls (HCs) was exploited to establish transcriptional signatures. Phenotypical and functional validation was performed in independent cohorts.

Results Transcriptome of cDC2s from patients with pSS revealed alterations in type I interferon (IFN), toll-like receptor (TLR), antigen processing and presentation pathways. Phenotypical validation showed increased CX3CR1 expression and decreased integrin beta-2 and plexin-B2 on pSS cDC2s. Functional validation confirmed impaired capacity of pSS cDC2s to degrade antigens and increased antigen uptake, including self-antigens derived from salivary gland epithelial cells. These changes in antigen uptake and degradation were linked to anti-SSA/Ro (SSA) autoantibodies and the presence of type I IFNs. In line with this, in vitro IFN-α priming enhanced the uptake of antigens by HC cDC2s, reflecting the pSS cDC2 profile. Finally, pSS cDC2s compared with HC cDC2s increased the proliferation and the expression of CXCR3 and CXCR5 on proliferating $CD4^+$ T cells.

Conclusions pSS cDC2s are transcriptionally altered, and the aberrant antigen uptake and processing, including (auto-)antigens, together with increased proliferation of tissue-homing $CD4^+$ T cells, suggest altered antigen presentation by pSS cDC2s. These functional alterations were strongly linked to anti-SSA positivity and the presence of type I IFNs. Thus, we demonstrate novel molecular and functional pieces of evidence for the role of cDC2s in orchestrating immune response in pSS, which may yield novel avenues for treatment.

WHAT IS ALREADY KNOWN ON THIS TOPIC

⇒ Type 2 conventional dendritic cells (cDC2s) are central in the initiation and control of immune responses, but their functional role in primary Sjögren's syndrome (pSS) is poorly understood.

WHAT THIS STUDY ADDS

⇒ Transcriptomic profile of cDC2s reveals changes in important pathways in patients with pSS consistent with cell activation, presence of type I interferon (IFN) and altered antigen response.
⇒ Phenotypical validation shows increased fractalkine receptor (CX3CR1) expression on cDC2s from patients with pSS.
⇒ cDC2s from patients with pSS with anti-Ro/SSA autoantibodies demonstrate altered antigen uptake and processing, modulated by type I IFN.
⇒ cDC2s from patients with pSS activate and increase CXCR3 and CXCR5 expression on $CD4^+$ T cells, facilitating migration to the inflammatory sites.

HOW THIS STUDY MIGHT AFFECT RESEARCH, PRACTICE OR POLICY

⇒ Considering their key role in orchestrating inflammatory responses understanding the underlying molecular mechanisms that drive cDC2 function and activation may disclose novel targets to halt immunopathology in pSS.

INTRODUCTION

Primary Sjögren's syndrome (pSS) is a systemic autoimmune disease characterised by prominent T-lymphocyte and B-lymphocyte infiltrations of the exocrine glands, which is associated with glandular destruction and dysfunction.[1 2] The immunological hallmarks of pSS include B-cell hyperactivity, the presence of anti-SSA/Ro (SSA) and anti-SSB/La antibodies[3] and a type I interferon (IFN) signature. Furthermore, the presence of a type I IFN signature in patients with pSS is associated with higher disease activity and higher levels of autoantibodies[4] and reinforces the involvement of the innate immune system.[5]

Type 2 conventional dendritic cells (cDC2s) are professional antigen-presenting cells with a unique ability to induce potent T-cell and B-cell responses.[6] On stimulation, cDC2s take up antigens and migrate into the T-cell area of the draining lymph node to initiate immune responses.[7] The internalisation, processing and presentation of antigens are a critical step for

T-cell priming. cDC2s are potent activators of $CD4^+$ T cells and induce T helper (Th) cell polarisation, thus directing the immune system in distinct directions.[8] Moreover, cDC2s can affect B-cell differentiation and survival, mainly through the production of B-cell activating factor (BAFF) and a proliferation-inducing ligand.[9] Activation and maturation of cDC2s to initiate adaptive immune responses can be potently amplified by inflammatory mediators, particularly type I IFNs.[10 11]

Despite the important role of cDC2s to activate T and B cells, their contribution to pSS immunopathology has been poorly studied. Recently, transcriptomic analysis of minor salivary glands from patients with pSS confirmed the presence of a cDC2 gene signature in the inflamed salivary glands, which was strongly associated with $CD4^+$ T cells.[12 13] In patients with pSS, cDC2s are epigenetically altered with decreased miR-130a expression and increased expression of its target mitogen- and stress-activated protein kinase-1, important for proinflammatory cytokine production. Furthermore, on stimulation, cDC2s from patients with pSS produce more interleukin (IL)-12 and tumour necrosis factor alpha (TNF-α).[14] In addition, in non-obese diabetic (NOD) and IQI/Jic, both spontaneous mouse models of Sjögren's syndrome, dendritic cell (DC) influx precedes the presence of focal lymphocytic infiltrates into the submandibular glands.[15 16] Furthermore, in aged mice lacking *Dcir* expression, a crucial negative regulator of DC function, mice spontaneously develop sialadenitis with elevated serum autoantibodies levels including anti-SSA, anti-SSB/La and antinuclear antibodies.[17] Thus, cDC2s seem to play an important role in pSS pathogenesis as well as in T-cell and B-cell activation and in driving salivary gland inflammation.

Here, we set out to investigate the role of cDC2s in pSS by exploiting RNA sequencing (RNAseq) to identify the transcriptional profile of circulating cDC2s from patients with pSS and non-Sjögren's sicca (nSS) as compared with healthy controls (HCs). In addition, we performed phenotypical and functional validation to confirm identified altered pathways and mechanisms through which cDC2s could drive pSS.

MATERIALS AND METHODS

Patients and controls

Patients and controls were age-matched and gender-matched and randomly allocated across the different experiments. All patients with pSS fulfilled the American-European Consensus Group (AECG) classification criteria for pSS.[18] Patients who did not fulfil the pSS classification criteria but presented with dryness complaints without a known cause in the absence of any generalised autoimmune disease were classified as patients with nSS and subjected to minor salivary gland biopsy. Two independent cohorts were selected to establish the transcriptional profile of cDC2s: a discovery cohort (14 with pSS, 9 with nSS and 8 HCs) and a replication cohort (9 with pSS, 6 with nSS and 10 HCs) (table 1). For the validation experiments, additional independent cohorts of HCs and patients with pSS were recruited (online supplemental table 1).

Patients and public involvement

Patients and HCs recruited for this study were not involved in the design, conduct, reporting or dissemination plans of our research.

Detailed information for all the methods, including phenotypical and functional validation, can be found in the online supplemental material and methods.

Table 1 Characteristics of the patients and controls enrolled in the RNAseq cohort

	RNAseq profiling					
	Discovery cohort (n=31)			Replication cohort (n=25)		
	HC	nSS	pSS	HC	nSS	pSS
N (M/F)	8 (0/8)	9 (0/9)	14 (3/11)	10 (1/9)	6 (0/6)	9 (1/8)
Age (years)	58 (54–67)	43 (26–68)	54 (29–70)	51 (29–59)	46 (24-68)	55 (26–76)
LFS (foci/4 mm^2)	–	0 (0.0–1.0)	1.9 (1.0–4.0)	–	0.1 (0.0–0.5)	2.1 (1.0–4.0)
ESSDAI	–	–	2.0 (0.0–19)	–	–	5.0 (1.0–13)
ESSPRI	–	–	3.7 (2.0–8.8)	–	–	2.9 (1.0–8.0)
Schirmer (mm/5 min)	–	3.3 (0.0–21)	5.0 (0.5–25)	–	10 (0.0–32)	13 (1.0–28)
ANA, n positive (%)	–	1 (11)	10 (71)	–	3 (50)	6 (67)
SSA, n positive (%)	–	2 (22)	8 (57)	–	2 (40)	5 (56)
SSB, n positive (%)	–	0 (0)	4 (29)	–	0 (0)	2 (22)
RF, n positive (%)	–	0 (0)	5 (42)	–	0 (0)	4 (50)
Serum IgG (g/L)	–	12 (6.8–17.0)	14 (8.3–30.0)	–	13 (11–15)	14 (8.5–42.0)
ESR (mm/hour)	–	11 (4.0–17.0)	11 (5.0–36.0)	–	7 (5.0–23.0)	14 (7.0–77.0)
C3 (g/L)	–	1.2 (0.6–2.0)	1.1 (0.7–1.3)	–	1.1 (0.8–1.3)	1.1 (0.5–1.6)
C4 (g/L)	–	0.3 (0.2–0.4)	0.3 (0.1–0.3)	–	0.2 (0.1–0.4)	0.3 (0.1–0.4)
Not treated, n (%)	–	6 (86)	11 (79)	–	6 (100)	6 (67)
Only HCQ, n (%)	–	1 (14)	1 (7)	–		1 (11)
Other, n (%)	–	–	2 (14)	–		2 (22)

Other treatment group includes, for discovery: azathioprine (n=1) and mesalazine (n=1), and for replication: azathioprine (n=1) and prednisone in combination with HCQ (n=1). Values are median unless stated otherwise.
ANA, antinuclear antibody; CRP, C reactive protein; ESR, erythrocyte sedimentation rate; ESSDAI, EULAR Sjögren's Syndrome Disease Activity Index; ESSPRI, EULAR Sjögren's Syndrome Patient-Reported Index; F, female; HC, healthy control; HCQ, hydroxychloroquine; LFS, Lymphocyte Focus Score; M, male; nSS, non-Sjögren's sicca; pSS, primary Sjögren's syndrome; RF, rheumatoid factor; RNAseq, RNA sequencing; SSA, anti-SSA/Ro; SSB, anti-SSB/La.

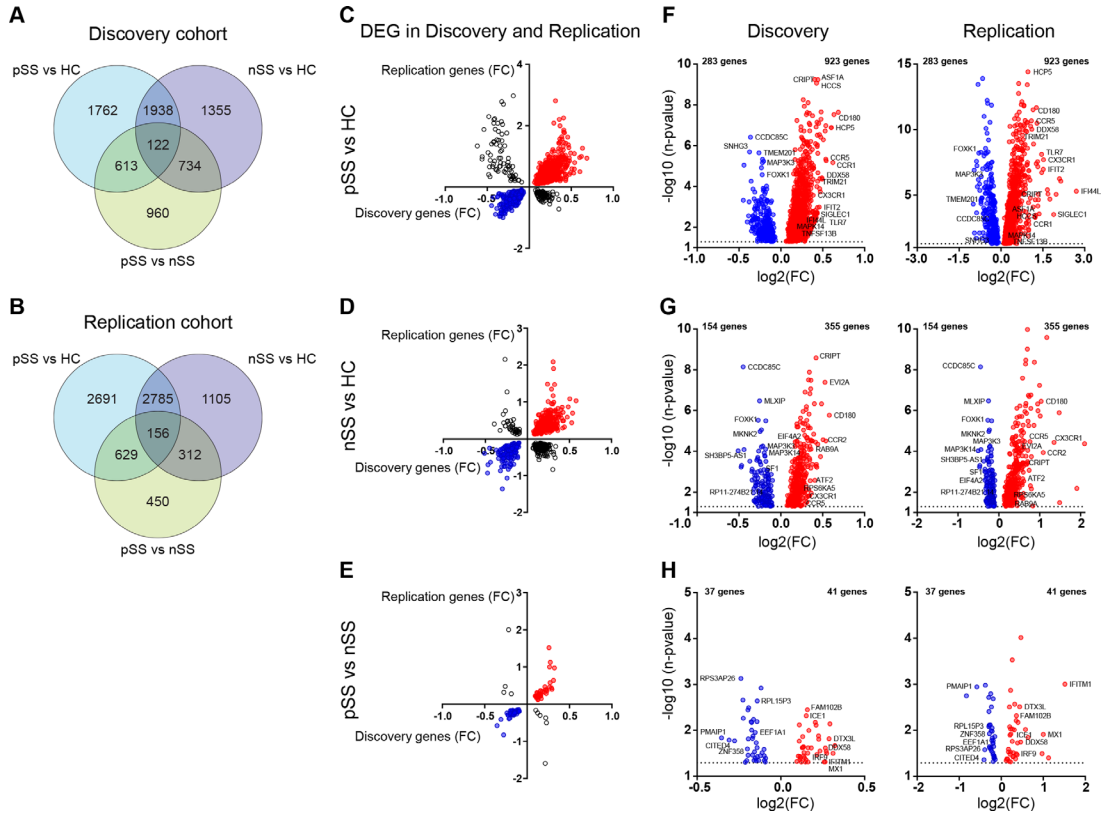

Figure 1 Transcriptomic characterisation of circulating cDC2s from patients with pSS and nSS. RNA sequencing of circulating cDC2s was performed independently for both discovery and replication cohorts. Venn diagrams show the overlap of the DEGs with a nominal p value of <0.05 between any of the three groups for the discovery cohort (A) and the replication cohort (B). Scatter plots show the FC (log2) of the DEGs between the two cohorts for the different comparisons, pSS versus HC (C), nSS versus HC (D) and pSS versus nSS (E). Volcano plots display the relationship between the FC (log2, x-axis) and the nominal p value (−log10, y-axis) of the DEGs consistently downregulated or upregulated in both cohorts for each comparison (F–H). cDC2, type 2 conventional dendritic cell; DEG, differentially expressed gene; FC, fold change; HC, healthy control; nSS, non-Sjögren's sicca; pSS, primary Sjögren's syndrome.

RESULTS

Transcriptome of cDC2s from patients with pSS is distinct from patients with nSS and HCs

In the discovery cohort, the majority of differentially expressed genes (DEGs) were found between pSS and HC cDC2s (figure 1A). Similarly, in the replication cohort, the larger number of DEG was also observed between pSS and HC cDC2s (figure 1B). In addition, cDC2s from patients with nSS partly exhibited changes in gene expression similar to pSS cDC2s in both cohorts. However, the magnitude of differences was generally larger in cDC2s from patients with pSS compared with patients with nSS. Overall, the cDC2 transcriptomic profile of patients with pSS overlaps to some extent to patients with nSS, but both are distinct from HCs (figure 1A,B).

To identify the most robust and consistently altered genes, those genes differentially expressed with a nominal p value of <0.05, with an average base mean expression (defined as the mean of normalised counts of all samples normalising for sequencing depth) higher than 100 in both cohorts, were selected (figure 1C–E). Of the DEGs identified in both cohorts, a large fraction (87% in pSS vs HC, 66% in nSS vs HC and 87% in nSS vs pSS) exhibited the same directionality (figure 1F–H) and therefore was considered to be replicated. The majority of the replicated DEGs were found between pSS and HC, and out of these, 30% (356 genes) were differentially expressed between nSS and HC (online supplemental figure 2). For the DEGs between patients with nSS and HC cDC2s, functional annotation did not reveal enriched pathways (online supplemental figure 3A). As for the DEGs between pSS versus nSS (figure 1H), functional annotation indicated that these genes were associated with viral and IFN-related pathways, nonsense-mediated decay and translation processes (online supplemental figure 3B-C).

Transcriptomic analysis of pSS cDC2s reveals impaired expression of genes involved in cell trafficking and activation

To gain further insight into the pSS cDC2s transcriptional profile, we identified the top 100 DEGs in both cohorts, based on fold-change differences. The majority of upregulated genes identified in pSS cDC2s included IFN-inducible genes (eg, *MX1*, *IFITM1* and *DDX58*) and molecules involved in cell migration (eg, *CCR2*, *CX3CR1* and *CCR5*) and activation (*TLR7*). Likewise, the top downregulated genes in pSS cDC2s comprise important regulators of cell activation like *NFKBIA*, a member of the nuclear factor kappa B (NF-κB) inhibitor family; *PLXNB2* and *PLXND1*, both negative regulators of IL-12p40 production[19]; *ITGB2*, a negative regulator of toll-like receptor (TLR) activation[20]; and *PELI1*, which negatively regulates non-canonical NF-κB signalling[21] (figure 2A).

As DC migration, cell–cell interaction and activation are crucial steps in the initiation and regulation of the immune

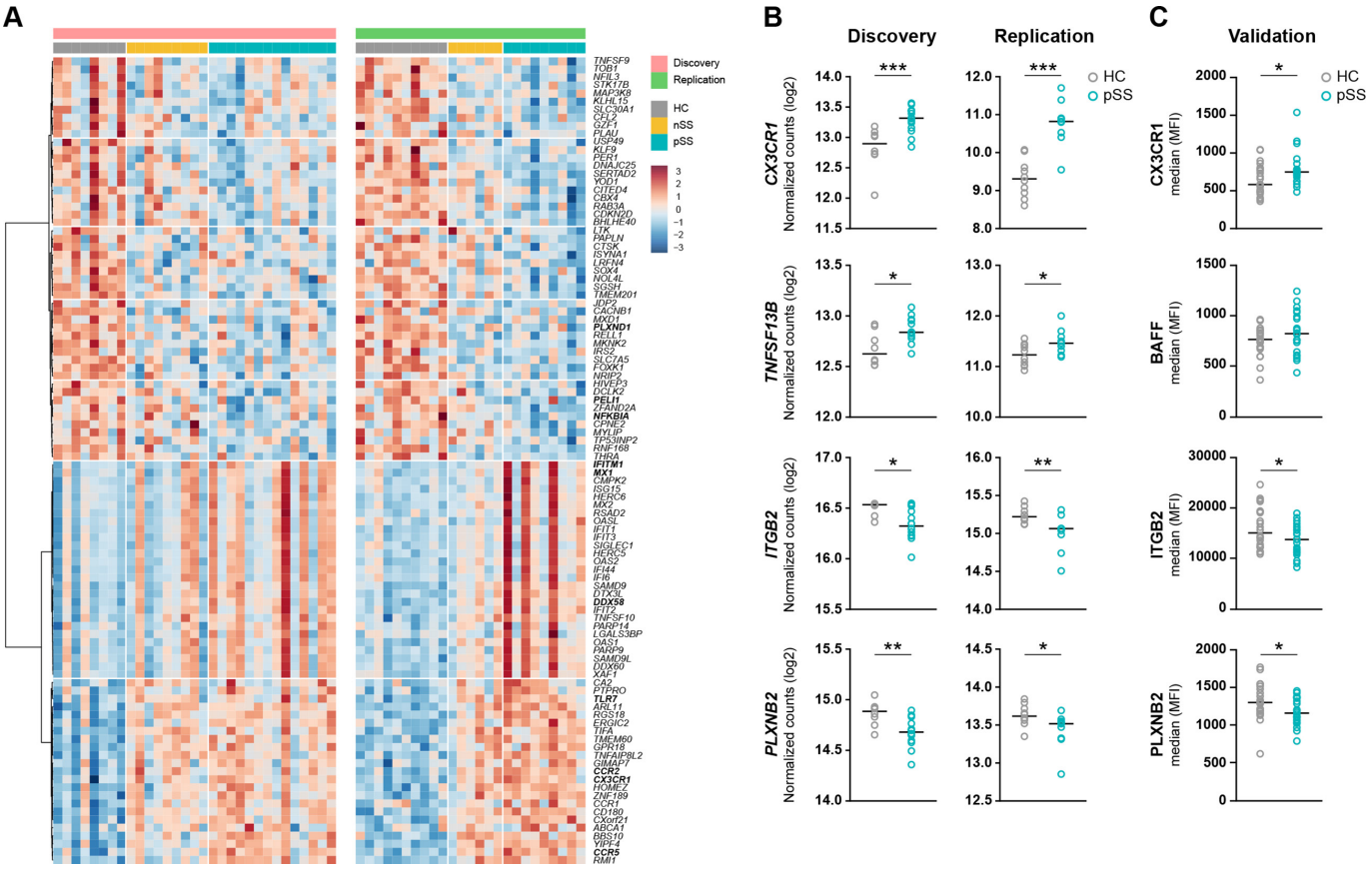

Figure 2 Transcriptomic profile and protein validation of cDC2s from patients with pSS display altered expression of key molecules involved in cell trafficking, activation and interferon signalling. Heatmap visualisation of the top 100 DEGs (50 upregulated and 50 downregulated genes, rows) across the two cohorts (discovery and replication) and the studied groups (HC, nSS and pSS; columns) clustered by Euclidean distance and Ward's method (A). Dot plots depict the expression of selected DEGs in discovery and replication cohorts in both HCs and patients with pSS (B). Protein expression of the selected DEGs was assessed on cDC2s by flow cytometry in HCs (n=22) and patients with pSS (n=22) (C). *, ** and *** represent nominal p values of <0.05, <0.01 and <0.001, respectively. cDC2, type 2 conventional dendritic cell; DEG, differentially expressed gene; HC, healthy control; nSS, non-Sjögren's sicca; pSS, primary Sjögren's syndrome.

response, we sought to further investigate the expression of potential mediators of these processes at protein level (figure 2B and online supplemental figure 4A). To this end, the protein expression of *CX3CR1*, a key chemokine receptor involved in trafficking of cDC2s,[22] *TNFSF13B* (BAFF), integrin beta-2 (*ITGB2*) and plexin-B2 (*PLXNB2*), both regulators of cell activation, was assessed by flow cytometry. In line with the transcriptomic data, the surface expression of CX3CR1 was significantly higher and the expression of ITGB2 and PLXNB2 was significantly lower on cDC2s from patients with pSS when compared with HCs. BAFF surface expression was not significantly different (figure 2C). Together, these results corroborate transcriptional changes in key mediators of migration and activation in pSS cDC2 and identify a possible mediator of cDC2 recruitment to the inflamed salivary glands.

To further understand the functional pathways altered in pSS cDC2s, we performed annotation of the consistent DEGs (figure 1F). Pathways involved in inflammation, including IFN signalling, class I major histocompatibility complex (MHC)-mediated antigen processing and presentation, TLR cascade and mitochondrial translation were enriched in pSS cDC2s compared with HC cDC2s (figure 3A). As TLRs are crucial receptors for cDC2 activation, we sought to investigate the phosphorylation profile of downstream TLR signalling mediators. However, we did not observe changes in the phosphorylation profile of p38, ERK1/2, JNK, ATF2 and NF-kB p65 between pSS cDC2s and HC cDC2s, both ex vivo and after TLR4 activation (online supplemental figure 5).

cDC2s from patients with pSS display a less effective antigen processing capacity

Antigen uptake and processing are crucial pathways in cDC2s that affect their antigen presentation to $CD4^+$ and $CD8^+$ T cells. As functional annotation of pSS cDC2 DEGs indicated altered antigen processing in pSS cDC2s, we performed in vitro validation experiments to assess the capacity of pSS cDC2s to degrade phagocytosed protein. To this end, we used bovine serum albumin (BSA) as an antigen model labelled with a fluorescent BODIPY dye (DQ-BSA). DQ-BSA is not fluorescent due to self-quenching, but on endocytosis and degradation, the self-quenching is abolished and a fluorescent signal can be detected using flow cytometry (figure 3B). As immunosuppressive treatment affects antigen processing, patients who were on treatment at the time of sample collection were excluded from this analysis (online supplemental figure 6A). We observed significantly reduced antigen processing in cDC2s from patients with pSS as compared with HCs, particularly at t=60 min (figure 3C–D). Next, we investigated the association between the presence of anti-SSA autoantibodies and the antigen processing

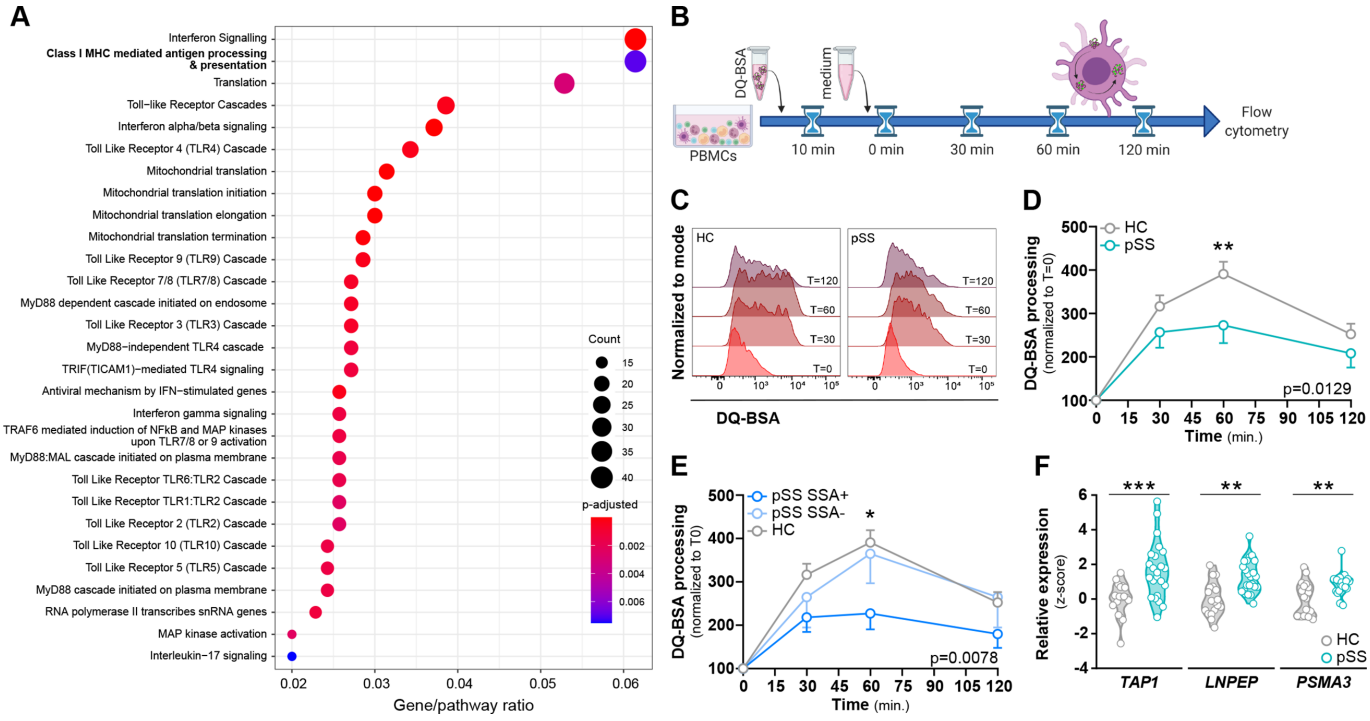

Figure 3 cDC2s from patients with pSS are functionally different in interferon-associated pathways and in antigen processing. Reactome pathway enrichment analysis was used for functional annotation of the DEGs between pSS versus HC (selected in figure 1F). The top significantly enriched reactome pathways are depicted. The x-axis shows the number of DEGs found within the pathway over the total number of pathway components (ratio); dot size depicts the number of genes used for enrichment and colour indicates the statistical significance (A). Isolated PBMCs were incubated with DQ–BSA for 10 min and antigen processing was followed for the indicated time points (B). Representative histograms (C) and quantification (D) of processed DQ-BSA, represented as MFI normalised to T=0, in HC (n=11) and non-treated patients with pSS (n=6) at different time points determined by flow cytometry. Quantification of DQ-BSA processing in patients with pSS with (pSS-SSA+, n=4) or without (pSS-SSA−, n=2) anti-SSA antibodies (E). Violin plots depict *TAP1*, *LNPEP* and *PSMA3* gene expressions in HC and patients with pSS from discovery and replication cohorts combined (F). cDC2, type 2 conventional dendritic cell; DEG, differentially expressed gene; DQ-BSA, fluorescent BODIPY dye labelled bovine serum albumin HC, healthy control; MFI, median fluorescence intensity; PBMC, peripheral blood mononuclear cell; pSS, primary Sjögren's syndrome.

capacity of cDC2s. Interestingly, cDC2s from patients with pSS with anti-SSA autoantibodies (pSS-SSA+) displayed a significantly lower processing capacity compared with HC, while patients without anti-SSAautoantibodies (pSS-SSA−) demonstrated antigen processing similar to that of HC (figure 3E). No differences were found in the frequency of circulating cDC2s between patients with pSS and HCs (online supplemental figure 4B).

As decreased capacity to process antigen has been associated with prolonged antigen survival, facilitating MHC-I supply,[23] and enhanced cross-presentation to $CD8^+$ T cells, we further investigated the expression of genes involved in class I-mediated processing. The expression of *TAP1*, a key transporter associated with MHC-I loading,[24] the peptidase *LNPEP*, implicated in endosomal trimming of cross-presented peptides and interaction with MHC-I molecules,[25] as well as the expression of proteasome subunits like *PSMA3*, involved in protein degradation in a ubiquitin-independent manner, were upregulated in cDC2s from patients with pSS compared with HCs (figure 3F). Thus, our results suggest that pSS cDC2s are possibly more efficient at storing (auto-) antigens, enhancing cross-presentation to $CD8^+$ T cells.

Increased antigen uptake of pSS cDC2s is related with anti-SSA autoantibodies and type I IFNs

As cDC2 antigen processing and presentation are importantly impacted by antigen uptake, we next investigated the capacity of cDC2s from patients with pSS and HCs to uptake BSA (figure 4A–B). Time-course analyses of BSA uptake demonstrated that pSS cDC2s have an increased antigen uptake compared with HC cDC2s, particularly at later time points (t=60 and t=120 min) (figure 4C). No differences were observed in cDC2 antigen uptake between patients who were treated with immune-suppressive treatment and those who were not (online supplemental figure 6B). Interestingly, cDC2s from pSS-SSA+ uptake more antigen compared with pSS-SSA− and HCs. A significantly higher uptake capacity was observed in pSS-SSA+ compared with HCs at t=60 min, and this further increased at t=120 min (figure 4D). In addition, at t=120 min, pSS-SSA+ cDC2s uptake more antigen compared with pSS-SSA−, who show similar BSA uptake to HC (figure 4D).

Given the strong association between the presence of anti-SSAautoantibodies and the IFN signature,[26] we confirmed that the majority of the pSS-SSA+ patients (8 out of 10) exhibited an IFN signature (pSS-IFN+), reflected by a higher IFN score (figure 4E). In addition, as functional annotation of DEGs in pSS cDC2s indicated altered IFN signalling, we investigated whether the presence of type I IFN affects cDC2 antigen uptake and processing. For this, HC cDC2s were left untreated or primed with IFN-α for 3 hours to mimic the IFN-signature and next challenged with labelled BSA (figure 4F). IFN-α priming of HC cDC2s increased antigen uptake by HC cDC2s to similar levels as those seen for pSS-SSA+ cDC2s (figure 4G) but did not alter antigen processing of cDC2s (data not shown). In addition, an increased antigen uptake was also observed in cDC2s from pSS-IFN+ patients compared with pSS-IFN− patients, particularly at

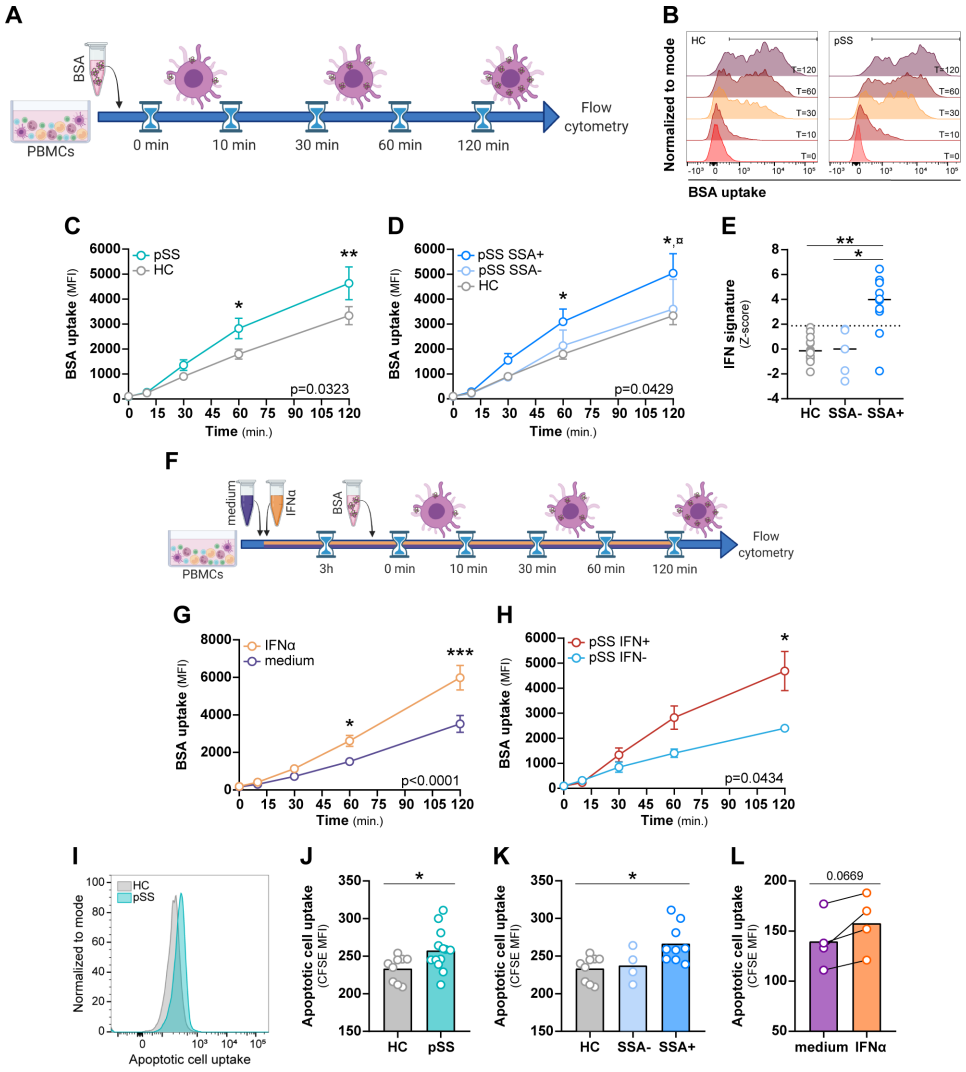

Figure 4 Enhanced uptake of antigen and apoptotic cells by pSS cDC2s is associated with autoimmunity and type I IFN. PBMCs from HC and patients with pSS were incubated with AF647–BSA for the indicated time points and the uptake by cDC2s, represented as MFI, was assessed by flow cytometry (A). Representative histograms (B) and quantification of BSA uptake by cDC2s of HCs (n=11) and patients with pSS (n=14) (C) and patients with pSS with (pSS-SSA+, n=10) or without (pSS-SSA–, n=4) anti-SSA antibodies (D). IFN signature calculated as the mean Z-score of five IFN-induced genes was determined by qPCR in HC (n=13), pSS-SSA– (n=5) and pSS-SSA+ (n=10) (E). HC-PBMCs were primed for 3 hours without (medium) or with IFN-α, exposed to AF647–BSA and chased for the indicated times by flow cytometry (F). The effect of IFN-α priming on BSA uptake was analysed in HC cDC2s (n=5) by flow cytometry (G). Quantification of BSA uptake by cDC2s of patients with pSS with (pSS-IFN+, n=9) or without (pSS-IFN–, n=3) IFN signature (H). Apoptotic CFSE labelled HSG-epithelial cells were added to PBMCs from HCs (n=9) and patients with pSS (n=13) at a 1:1 ratio for 120 min. Representative histogram (I) and quantification of apoptotic cell uptake of cDC2s from HCs and patients with pSS (J) and pSS-SSA– (n=4) and pSS-SSA+ (n=9) (K) measured by flow cytometry. HC-PBMCs were primed for 3 hours with IFN-α or without (medium) and exposed to apoptotic CFSE labelled HSG-epithelial cells for 2 hours. The effect of IFN-α priming on apoptotic cell uptake was analysed in HC cDC2s (n=4) by flow cytometry (L). Results are represented as mean±SEM. *, ** and *** represent p values of <0.05, <0.01 and <0.001, respectively. cDC2, type 2 conventional dendritic cell; HC, healthy control; HSG, human salivary gland; IFN, interferon; MFI, median fluorescence intensity; PBMC, peripheral blood mononuclear cell; pSS, primary Sjögren's syndrome; qPCR, quantitative PCR.

t=120 min (figure 4H). Together, these results show that cDC2s from anti-SSA+ patients with pSS have an increased antigen uptake capacity related to the IFN signature, as exposure of HC cDC2s to type I IFN induces an increase uptake profile similar to pSS-SSA+ cDC2s.

Next, we tested whether pSS-SSA+ cDC2s also uptake increased amounts of autoantigens derived from apoptotic human salivary gland (HSG)-epithelial cells, which is a relevant mechanism to drive pSS. To this end, PBMCs from patients with pSS and HC were incubated with apoptotic carboxyfluorescein succinimidyl ester (CFSE)-labelled HSG-epithelial cells for 2 hours, and the phagocytic capacity of cDC2s was assessed by flow cytometry (online supplemental figure 7). Similar to BSA uptake, pSS cDC2s displayed a significantly enhanced ability to uptake apoptotic HSG-epithelial cells (figure 4I–J) compared with HC cDC2s. Furthermore, the increased uptake of apoptotic HSG-epithelial cells was only observed in cDC2s of pSS-SSA+ patients (figure 4K). Moreover, IFN-α priming of HC cDC2s increased uptake of apoptotic HSG-epithelial cells by HC cDC2s, as observed in BSA uptake, although without statistical significance (figure 4L). Thus, cDC2s from patients with pSS with anti-SSA antibodies also uptake autoantigens more efficiently, possibly associated with the presence of type I IFN.

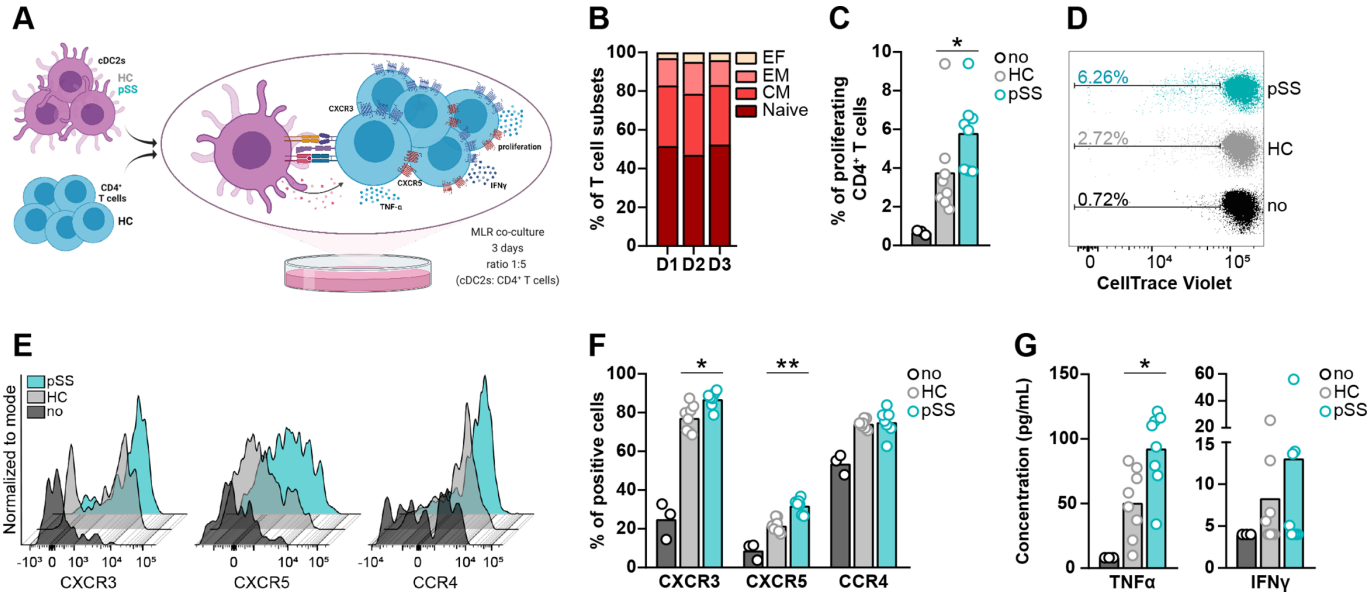

Figure 5 cDC2s from patients with pSS efficiently induce CD4$^+$ T-cell proliferation with a tissue homing signature. Total CD4$^+$ T cells from HCs were cultured alone (n=3) or cocultured either with cDC2s from HCs (n=3) or patients with pSS (n=3) at a 5:1 ratio (T cells:cDC2s) for 3 days (A). The frequency of CD4$^+$ T-cell subsets (naïve; CM, EM and EF) was assessed by flow cytometry directly after cell isolation (B). Quantification (C) and representative flow cytometry dot plot (D) of proliferating CD4$^+$ T cells measured by flow cytometry at day 3. Representative histograms of CXCR3, CXCR5 and CCR4 expression on proliferating CD4$^+$ T cells (E) and quantification of the percentage of chemokine receptor expressing CD4$^+$ T cells measured by flow cytometry (F). TNF-α and IFN-γ production during T cells: cDC2s coculture was measured by ELISA (G). cDC2, type 2 conventional dendritic cell; CM, central memory; EF, effector; EM, effector memory; HC, healthy control; IFN-γ, interferon gamma; pSS, primary Sjögren's syndrome; TNF-α, tumour necrosis factor alpha.

pSS cDC2s increase proliferation of CD4$^+$ T cells with a tissue homing signature

In the context of the enhanced antigen uptake observed in pSS cDC2s, we next evaluated whether in vivo priming by these cells differently affects CD4$^+$ T-cell activation in vitro. CD4$^+$ T cells from HCs were allogenic cocultured with cDC2s from either patients with pSS or HCs for 3 days (figure 5A). No significant differences were observed among the CD4$^+$ T-cell subsets between the different donors at the start of the experiment (figure 5B and online supplemental figure 8A). Coculture of CD4$^+$ T cells with pSS cDC2s significantly increased the frequency of proliferating CD4$^+$ T cells compared with coculture with HC cDC2s (figure 5 C-D, and online supplemental figure 8B). In addition, we observed an increased percentage of proliferating CD4$^+$ T cells expressing CXCR3 and CXCR5 in the presence of pSS cDC2s when compared with HC cDC2s. No differences were observed on CCR4 expression (figure 5E–F). Furthermore, CD4$^+$ T cells cocultured with pSS cDC2s produced substantially increased levels of TNF-α but not IFN-γ (figure 5G). Thus, the altered transcriptional profile and observed differences in antigen uptake and processing in pSS cDC2s are associated with an increased capacity to activate CD4$^+$ T cells to express markers that allow them to migrate to the salivary glands and produce proinflammatory cytokines to drive local autoimmune response.

DISCUSSION

In-depth transcriptional profiling was performed in two independent cohorts and identified consistent transcriptional alterations in cell trafficking, activation, IFN signalling and class I-mediated antigen processing and presentation in cDC2s from patients with pSS compared with patients with nSS and HCs. Using in vitro cultures with primary isolated cDC2s from patients with pSS, we confirmed that pSS cDC2s display altered uptake and processing of (auto-)antigens. We observed that these differences were most pronounced in patients with pSS with anti-SSA antibodies, linked with type I IFN and possibly associated with enhanced antigen presentation to CD4$^+$ and CD8$^+$ T cells. Indeed, pSS cDC2s mediated increased proliferation of CD4$^+$ T cells, associated with increased expression of chemokine receptors and enhanced production of TNF-α.

Our transcriptomic analysis revealed that the altered molecular signature found in cDC2s from patients with pSS is, at least in part, shared by cDC2s from patients with nSS. Although patients with nSS do not display signs of systemic autoimmune disease, this heterogeneous group of patients shares severe objective dryness and occasionally presents single systemic features similar to patients with pSS. The overlap of clinical features and DEGs between pSS and nSS suggests that patients with nSS might have a low-grade inflammatory environment similar to patients with pSS and thus might share immune mediated pathological processes driving symptom burden. In accordance, we previously showed that the transcriptomic profile of plasmacytoid dendritic cells and monocytes of patients with nSS display an intermediate phenotype that largely overlaps with that of patients with pSS.[27 28] In addition, patients with nSS also share locally and systemically signs of immune activation with patients with pSS such as presence of effector T cells (Th1, Th17 and Tfh cells) in the salivary glands and similar proteomic profile and increased circulating U6-sncRNA in circulation.[29–31] However, differences in IFN signalling and nonsense-mediated decay pathways in cDC2s of patients with nSS could indicate that these patients still maintain some regulatory mechanisms to ensure cellular homeostasis.[32] Altogether, the transcriptional profile of patients with nSS reveals an intermediate phenotype between HCs and patients with pSS. As such, longitudinal studies and further investigation in the regulation of the immune profile of patients with nSS are essential to gain more insight into the

mechanisms driving immune activation and development of pSS immunopathology.

The presence of cDC2s in the salivary glands of patients with pSS is clear[12 13]; however, the mechanisms that regulate the migration of cDC2s to the inflamed glands are unknown. Given the increased CX3CR1 expression in pSS cDC2s and since fractalkine levels (CX3CL1, the CX3CR1 ligand) are increased in the salivary gland of patients with pSS,[33] the CX3CL1–CX3CR1 axis could mediate the presence of cDC2s in the inflamed glands of patients with pSS. In fact, recruitment and adhesion of CX3CR1-expressing cDC2s mediated by fractalkine lead to their accumulation in inflamed kidneys.[22] Furthermore, reduction of PLXNB2, a negative regulator of IL-12/IL-23p40 response,[19] is in line with increased IL-12 levels found in patients with pSS.[34] Hence, a reduction of PLXNB2 expression may contribute to increase IL-12 production in patients with pSS. Moreover, the decreased ITGB2 expression in pSS cDC2s is in accordance with an activated state of these cells, in view of its role as negative regulator of TLR activation[20] and mediator of T-cell priming by DC.[35] As such, the enhanced CX3CR1 expression combined with changes in cell-activating pathways indicates that cDC2s could significantly contribute to the maintenance and possibly the initiation of inflammatory responses in pSS.

The less efficient antigen processing observed in cDC2s from patients with pSS can possibly lead to long-term antigen storage, shown to occur in mature DCs.[36] This antigen retention capacity by cDC2s, together with their migratory profile, suggests that pSS cDC2s favour the coordination of an efficient antigen presentation/cross-presentation to T cells at specific inflammatory sites. Long-term antigen storage can promote more effective cross-presentation via MHC-I, which is in line with the increased *TAP1* and *LNPEP* expression observed in pSS cDC2s. These molecules can potentiate cross-presentation by enhancing the transport of antigen-derived peptides for binding to MHC-I[37] and by trimming peptides in optimal size for loading on MHC-I,[38] providing potent $CD8^+$ T-cell activation that in turn can contribute to exacerbate the immune inflammation in the salivary glands. Hence, the activated $CD8^+$ T cells present in the salivary glands of patients with pSS, which are associated with increased lymphocytic focus score, disease severity and autoimmunity,[39] can be, in part, a consequence of an impaired regulation of cross-presentation by cDC2s.

Type I IFNs are pleiotropic cytokines that can affect not only the maturation and activation of cDC2s[11] but also antigen-related processes. We showed that IFN-α priming increased the uptake capacity of HC cDC2s to levels observed in pSS-SSA+ patients and that impaired antigen processing was also related with type I IFNs. Although antigen processing by cDC2s remained unaltered after short IFN-α priming (3 hours), stimulation for 24 hours was effective to upregulate genes involved in class I antigen processing and cross-presentation in a subset of cDC2s,[11] suggesting that the modulation by IFN might be a long-lasting process. In line with this, IFN-α-driven monocyte-derived DCs were characterised by upregulation of genes linked to antigen processing and degradation, resembling cDC2 from patients with pSS with anti-SSA antibodies.[23 40] Thus, the auto-sustaining feedback loop that, in part, maintains IFN production and anti-SSA antibodies alters cDC2 functions and possibly cDC2s-mediated T-cell activation.

Apoptosis represents an important source of self-antigens for DCs, and it has recently emerged as a possible mechanism to expose autoantigens in pSS.[41 42] In fact, this process can trigger immune cell activation to self-proteins[43] as challenging of DCs with apoptotic cells induces their maturation, IL-12 production and Th1/Th17 responses.[44 45] Moreover, apoptosis of epithelial cells leads to cleavage and translocation of Sjögren's autoantigens, including α-fodrin and SSA, into apoptotic particles.[46] The increased uptake of apoptotic cells by cDC2s of anti-SSA+ patients with pSS could represent a mechanism through which cDC2s activate $CD4^+$ T cells and B cells to maintain the autoantibody production observed in pSS. Although the mechanisms underlying the antigen uptake and processing by pSS cDC2s need to be further clarified, our results suggest that these processes may be driven by type I IFN and could significantly contribute to the chronic inflammatory response observed in pSS.

Interestingly, the increased $CD4^+$ T-cell proliferation induced by pSS cDC2s with a tissue homing signature corroborates that cDC2s are also important in reshaping the $CD4^+$ T-migratory profile in pSS. Blocking of CXCR3 function in a NOD mouse model of pSS reduces effector $CD8^+$ T-cell infiltration and TNF-α expression in the salivary glands.[47] Moreover, the increased *CXCR5* expression induced by pSS cDC2s is in line with an increase frequency and recruitment to the salivary glands of patients with pSS, despite the differences observed in the peripheral blood.[29 48–50] Recruitment of CXCR5 expressing $CD4^+$ T cells is mediated by CXCL13 to ensure preferential B-cell interaction and activation.[51] In the salivary glands of patients with pSS, CXCR5-expressing Tfh cells strongly correlated with *CXCL13* expression and were associated with B-cell frequency and lymphocytic infiltration.[29] Thus, these findings suggest that pSS cDC2s, through the modulation of $CD4^+$ T-cell chemokine receptors, favour their migration to the salivary glands contributing to B-cell hyperactivity. However, whether $CD4^+$ T cells undergo expansion in the gland, or whether it occurs elsewhere, for example, in the lymphoid organs, with subsequent migration still remains unclear.

In conclusion, cDC2s from patients with pSS are transcriptionally altered, display an aberrant antigen uptake and processing, including self-antigens derived from salivary gland epithelial cells, and induce increased proliferation of tissue-homing $CD4^+$ T cells. Although our study has limitations related with sample size and heterogeneity of the RNAseq analysis cohorts, we were able to successfully corroborate these results using an independent set of patients with pSS and HC to experimentally validate our hypothesis. Future studies in larger cohorts of patients with integrated analysis of different multiomics data from different tissues would be valuable to support our study. These data represent the first evidence of molecular and functional alteration of cDC2s in pSS, highlighting a novel pathway via which cDC2s contribute to the pSS pathogenesis.

Correction notice This article has been corrected since it was first published. The open access licence has been updated to CC BY.

Acknowledgements We thank Dr Lynne Bingle for kindly providing the human submandibular salivary gland epithelial cell line (HTB-41). Schematic representations were created with BioRender (biorender.com).

Contributors APL, MRH, TRDJR and JAvR were involved in the conception and design of the study. APL, MRH, ACH, SLMB, CPJB and AAK were involved in data acquisition. APL, MRH, CPJB, AP, AAK, TRDJR and JAvR were involved in data analysis and interpretation. APL drafted the manuscript. All authors contributed to the article and approved the submitted version. APL and JAvR are responsible for the overall content as the guarantors.

Funding APL was supported by a PhD grant from the Portuguese national funding agency for science, research and technology: Fundação para a Ciência e a Tecnologia (SFRH/BD/116082/2016). TRDJR received research funding from GlaxoSmithKline (GSK) for his work on Sjögren's syndrome as part of the GSK Immune Catalyst Program. The funding sources had no role in study design; data collection, analysis, and interpretation; writing; or in the decision to submit the manuscript for publication.

Competing interests TRDJR was the principal investigator in the immune catalyst programme of GlaxoSmithKline, which was an independent research programme. He did not receive any financial support other than the research funding for the current project. Currently, He is an employee of Abbvie, where he holds stock. He had no part in the design and interpretation of the study results after he started at Abbvie. The remaining authors declare that the research was conducted in the absence of any commercial or financial relationships that could be construed as a potential conflict of interest.

Patient and public involvement Patients and/or the public were not involved in the design, conduct, reporting or dissemination plans of this research.

Patient consent for publication Not applicable.

Ethics approval This study involves human participants and was approved by the University Medical Center Utrecht (METC no. 13-697). The participants gave informed consent to participate in the study before taking part in accordance with the declaration of Helsinki.

Provenance and peer review Not commissioned; externally peer reviewed.

Data availability statement Data are available in a public, open access repository. The RNA sequencing datasets generated for this study can be found in NCBI's Gene Expression Omnibus under the following accession number GSE200020.

ORCID iDs
Ana P Lopes http://orcid.org/0000-0003-4954-5151
Aridaman Pandit http://orcid.org/0000-0003-2057-9737

REFERENCES

1 Ogawa Y, Shimizu E, Tsubota K. Interferons and dry eye in Sjögren's syndrome. *Int J Mol Sci* 2018;19:3548.
2 Brito-Zerón P, Baldini C, Bootsma H, *et al*. Sjögren syndrome. *Nat Rev Dis Primers* 2016;2:16047.
3 Shen L, Suresh L. Autoantibodies, detection methods and panels for diagnosis of Sjögren's syndrome. *Clin Immunol* 2017;182:24–9.
4 Bodewes ILA, Al-Ali S, van Helden-Meeuwsen CG, *et al*. Systemic interferon type I and type II signatures in primary Sjögren's syndrome reveal differences in biological disease activity. *Rheumatology* 2018;57:921–30.
5 Båve U, Nordmark G, Lövgren T, *et al*. Activation of the type I interferon system in primary Sjögren's syndrome: a possible etiopathogenic mechanism. *Arthritis Rheum* 2005;52:1185–95.
6 Rossi M, Young JW. Human dendritic cells: potent antigen-presenting cells at the crossroads of innate and adaptive immunity. *J Immunol* 2005;175:1373–81.
7 Sozzani S. Dendritic cell trafficking: more than just chemokines. *Cytokine Growth Factor Rev* 2005;16:581–92.
8 Yin X, Yu H, Jin X, *et al*. Human blood CD1c+ dendritic cells encompass CD5high and CD5low subsets that differ significantly in phenotype, gene expression, and functions. *J Immunol* 2017;198:1553–64.
9 Poudrier J, Chagnon-Choquet J, Roger M. Influence of dendritic cells on B-cell responses during HIV infection. *Clin Dev Immunol* 2012;2012:592187.
10 Longhi MP, Trumpfheller C, Idoyaga J, *et al*. Dendritic cells require a systemic type I interferon response to mature and induce CD4+ Th1 immunity with poly IC as adjuvant. *J Exp Med* 2009;206:1589–602.
11 Girard M, Law JC, Edilova MI, *et al*. Type I interferons drive the maturation of human DC3s with a distinct costimulatory profile characterized by high GITRL. *Sci Immunol* 2020;5. doi:10.1126/sciimmunol.abe0347. [Epub ahead of print: 13 11 2020].
12 Oyelakin A, Horeth E, Song E-AC, *et al*. Transcriptomic and network analysis of minor salivary glands of patients with primary Sjögren's syndrome. *Front Immunol* 2020;11:606268.
13 Cheng C, Zhou J, Chen R, *et al*. Predicted disease-specific immune infiltration patterns decode the potential mechanisms of long non-coding RNAs in primary Sjogren's syndrome. *Front Immunol* 2021;12:624614.
14 Lopes AP, van Roon JAG, Blokland SLM, *et al*. MicroRNA-130a contributes to type-2 classical DC-activation in Sjögren's syndrome by targeting mitogen- and stress-activated protein kinase-1. *Front Immunol* 2019;10:1335.
15 van Blokland SC, van Helden-Meeuwsen CG, Wierenga-Wolf AF, *et al*. Two different types of sialoadenitis in the Nod- and MRL/lpr mouse models for Sjögren's syndrome: a differential role for dendritic cells in the initiation of sialoadenitis? *Lab Invest* 2000;80:575–85.
16 Konno A, Takada K, Saegusa J, *et al*. Presence of B7-2+ dendritic cells and expression of Th1 cytokines in the early development of sialodacryoadenitis in the IQI/Jic mouse model of primary Sjörgren's syndrome. *Autoimmunity* 2003;36:247–54.
17 Fujikado N, Saijo S, Yonezawa T, *et al*. Dcir deficiency causes development of autoimmune diseases in mice due to excess expansion of dendritic cells. *Nat Med* 2008;14:176–80.
18 Vitali C, Bombardieri S, Jonsson R, *et al*. Classification criteria for Sjögren's syndrome: a revised version of the European criteria proposed by the American-European consensus group. *Ann Rheum Dis* 2002;61:554–8.
19 Holl EK, Roney KE, Allen IC, *et al*. Plexin-B2 and Plexin-D1 in dendritic cells: expression and IL-12/IL-23p40 production. *PLoS One* 2012;7:e43333.
20 Yee NK, Hamerman JA, beta HJA. β(2) integrins inhibit TLR responses by regulating NF-κB pathway and p38 MAPK activation. *Eur J Immunol* 2013;43:779–92.
21 Liu J, Huang X, Hao S, *et al*. Peli1 negatively regulates noncanonical NF-κB signaling to restrain systemic lupus erythematosus. *Nat Commun* 2018;9:1136.
22 Kassianos AJ, Wang X, Sampangi S, *et al*. Fractalkine-CX3CR1-dependent recruitment and retention of human CD1c+ myeloid dendritic cells by in vitro-activated proximal tubular epithelial cells. *Kidney Int* 2015;87:1153–63.
23 Spadaro F, Lapenta C, Donati S, *et al*. IFN-α enhances cross-presentation in human dendritic cells by modulating antigen survival, endocytic routing, and processing. *Blood* 2012;119:1407–17.
24 Gutiérrez-Martínez E, Planès R, Anselmi G, *et al*. Cross-presentation of cell-associated antigens by MHC class I in dendritic cell subsets. *Front Immunol* 2015;6:363.
25 Saveanu L, van Endert P. The role of insulin-regulated aminopeptidase in MHC class I antigen presentation. *Front Immunol* 2012;3:57.
26 Brkic Z, Maria NI, van Helden-Meeuwsen CG, *et al*. Prevalence of interferon type I signature in CD14 monocytes of patients with Sjogren's syndrome and association with disease activity and BAFF gene expression. *Ann Rheum Dis* 2013;72:728–35.
27 Hillen MR, Pandit A, Blokland SLM, *et al*. Plasmacytoid DCs from patients with Sjögren's syndrome are transcriptionally primed for enhanced pro-inflammatory cytokine production. *Front Immunol* 2019;10:2096.
28 Lopes AP, Bekker CPJ, Hillen MR, *et al*. The transcriptomic profile of monocytes from patients with Sjögren's syndrome is associated with inflammatory parameters and is mimicked by circulating mediators. *Front Immunol* 2021;12:701656.
29 Blokland SLM, van Vliet-Moret FM, Hillen MR, *et al*. Epigenetically quantified immune cells in salivary glands of Sjögren's syndrome patients: a novel tool that detects robust correlations of T follicular helper cells with immunopathology. *Rheumatology* 2020;59:335–43.
30 Pucino V, Turner JD, Nayar S, *et al*. Sjögren's and non-Sjögren's sicca share a similar symptom burden but with a distinct symptom-associated proteomic signature. *RMD Open* 2022;8.
31 Lopes AP, Hillen MR, Chouri E, *et al*. Circulating small non-coding RNAs reflect IFN status and B cell hyperactivity in patients with primary Sjögren's syndrome. *PLoS One* 2018;13:e0193157.
32 Nickless A, Bailis JM, You Z. Control of gene expression through the nonsense-mediated RNA decay pathway. *Cell Biosci* 2017;7:26.
33 Astorri E, Scrivo R, Bombardieri M, *et al*. Cx3Cl1 and CX3CR1 expression in tertiary lymphoid structures in salivary gland infiltrates: fractalkine contribution to lymphoid neogenesis in Sjogren's syndrome. *Rheumatology* 2014;53:611–20.
34 Chen X, Aqrawi LA, Utheim TP, *et al*. Elevated cytokine levels in tears and saliva of patients with primary Sjögren's syndrome correlate with clinical ocular and oral manifestations. *Sci Rep* 2019;9:7319.
35 Balkow S, Heinz S, Schmidbauer P, *et al*. Lfa-1 activity state on dendritic cells regulates contact duration with T cells and promotes T-cell priming. *Blood* 2010;116:1885–94.
36 van Montfoort N, Camps MG, Khan S, *et al*. Antigen storage compartments in mature dendritic cells facilitate prolonged cytotoxic T lymphocyte cross-priming capacity. *Proc Natl Acad Sci U S A* 2009;106:6730–5.
37 Kuchtey J, Chefalo PJ, Gray RC, *et al*. Enhancement of dendritic cell antigen cross-presentation by CpG DNA involves type I IFN and stabilization of class I MHC mRNA. *J Immunol* 2005;175:2244–51.
38 Saveanu L, Carroll O, Weimershaus M, *et al*. Irap identifies an endosomal compartment required for MHC class I cross-presentation. *Science* 2009;325:213–7.
39 Mingueneau M, Boudaoud S, Haskett S, *et al*. Cytometry by time-of-flight immunophenotyping identifies a blood Sjögren's signature correlating with disease activity and glandular inflammation. *J Allergy Clin Immunol* 2016;137:1809–21.
40 Parlato S, Romagnoli G, Spadaro F, *et al*. Lox-1 as a natural IFN-alpha-mediated signal for apoptotic cell uptake and antigen presentation in dendritic cells. *Blood* 2010;115:1554–63.
41 Katsiougiannis S, Tenta R, Skopouli FN. Endoplasmic reticulum stress causes autophagy and apoptosis leading to cellular redistribution of the autoantigens Ro/

Sjögren's syndrome-related antigen A (SSA) and La/SSB in salivary gland epithelial cells. *Clin Exp Immunol* 2015;181:244–52.
42 Tanaka T, Warner BM, Odani T, *et al*. LAMP3 induces apoptosis and autoantigen release in Sjögren's syndrome patients. *Sci Rep* 2020;10:15169.
43 Dixon KO, O'Flynn J, van der Kooij SW, *et al*. Phagocytosis of apoptotic or necrotic cells differentially regulates the transcriptional expression of IL-12 family members in dendritic cells. *J Leukoc Biol* 2014;96:313–24.
44 Fransen JH, Hilbrands LB, Ruben J, *et al*. Mouse dendritic cells matured by ingestion of apoptotic blebs induce T cells to produce interleukin-17. *Arthritis Rheum* 2009;60:2304–13.
45 Fransen JH, van der Vlag J, Ruben J, *et al*. The role of dendritic cells in the pathogenesis of systemic lupus erythematosus. *Arthritis Res Ther* 2010;12:207.
46 Ainola M, Porola P, Takakubo Y, *et al*. Activation of plasmacytoid dendritic cells by apoptotic particles - mechanism for the loss of immunological tolerance in Sjögren's syndrome. *Clin Exp Immunol* 2018;191:301–10.
47 Zhou J, Yu Q. Disruption of CXCR3 function impedes the development of Sjögren's syndrome-like xerostomia in non-obese diabetic mice. *Lab Invest* 2018;98:620–8.
48 Aqrawi LA, Ivanchenko M, Björk A, *et al*. Diminished CXCR5 expression in peripheral blood of patients with Sjögren's syndrome may relate to both genotype and salivary gland homing. *Clin Exp Immunol* 2018;192:259–70.
49 Dupré A, Pascaud J, Rivière E, *et al*. Association between T follicular helper cells and T peripheral helper cells with B-cell biomarkers and disease activity in primary Sjögren syndrome. *RMD Open* 2021;7.
50 Jin L, Yu D, Li X, *et al*. CD4+CXCR5+ follicular helper T cells in salivary gland promote B cells maturation in patients with primary Sjogren's syndrome. *Int J Clin Exp Pathol* 2014;7:1988–96.
51 Chevalier N, Jarrossay D, Ho E, *et al*. Cxcr5 expressing human central memory CD4 T cells and their relevance for humoral immune responses. *J Immunol* 2011;186:5556–68.

SUPPLEMENTARY MATERIAL AND METHODS

cDC2s isolation and RNA isolation

cDC2s were isolated from peripheral blood mononuclear-cells (PBMCs) by magnetic-activated cell sorting (MACS) using CD1c (BDCA-1)$^+$ Dendritic Cell Isolation Kit (Miltenyi Biotec) according to the manufacturer's instructions. In brief, CD19+ cells were depleted using anti-CD19-coated magnetic beads, and after CD1c+ cells were isolated using biotinylated anti-CD1c and anti-biotin-beads. cDC2s purity measured by flow cytometry (**Supplementary Table 2** and **Supplementary Figure 1**) was 90% [83–97%] (median [interquartile range]), and there were no significant differences between groups.

Cells were lysed in RLTplus buffer (Qiagen) supplemented with 1% beta-mercaptoethanol for transcriptional analyses. Total RNA was purified using AllPrep Universal Kit (Qiagen), according to the manufacturer's instructions. RNA concentration was assessed with Qubit RNA Kit (Thermo Fisher Scientific) and RNA integrity was measured by capillary electrophoresis using the RNA 6000 Nano Kit (Agilent Technologies); all samples had a RIN-score >7.0.

RNA sequencing analysis

RNA sequencing was performed at the Beijing genomics institute, at two different time points, using a NextSeq 500 sequencer (Illumina) for the discovery cohort and an Illumina HiSeq 4000 sequencer (Illumina) for the replication cohort, following the standard manufacturer's protocols. For both cohorts about 20 million paired-end (91 bp for discovery; 100 bp for replication) reads were generated for each sample. RNA-sequencing data analysis was performed as previously described [1]. Briefly, FastQC tool (https://www.bioinformatics.babraham.ac.uk/projects/fastqc/), was used to assess the quality control of the reads. All samples passed the quality check. Next, reads were aligned to the human genome assembly (GRCh38 build 79) [2] using STAR aligner [3]. The aligned reads (mapping quality > 30) were used to calculate the read counts using Python package HTSeq [4] for each annotated gene. To remove unwanted variance (k=1 parameter) related with technical aspects RUVSeq was used [5]. A total of 65217 genes were analyzed in both cohorts. Differentially expressed genes (DEGs) were identified using Bioconductor/R package DESeq2 [6]; Wald's test was used to identify DEGs in each pair-wise comparison performed

between the three groups (HC, nSS, and pSS) and likelihood ratio test to identify DEGs considering multiple groups. Differences in gene expression with a nominal p-value <0.05 were considered differentially expressed. Variance stabilizing transformation was applied to obtain normalized gene counts (variance stabilized data), which were used for subsequent analyses. Raw and processed RNA sequencing data are available in NCBI's Gene Expression Omnibus under the following accession number GSE200020.

Pathway enrichment analysis

Pathway enrichment analysis, was performed for the consistently DEGs in both cohorts using the R/Bioconductor package ReactomePA [7] to identify the processes and pathways dysregulated between patients and HC.

Flow cytometry

For validation of the selected targets identified by RNA sequencing, PBMCs were cryopreserved in complete medium (RPMI glutamax (Thermo Fisher Scientific) supplemented with 10% heat-inactivated FCS (Sigma-Aldrich) and 1% penicillin/streptomycin (Thermo Fisher Scientific)) and freezing medium (20% (v/v) DMSO in FCS) at a 1:1 ratio. PBMCs were thawed and washed prior to incubation with the fixable viability dye eFluor506 (eBioscience) to allow exclusion of dead cells and blocked with Fc receptor blocking reagent (Miltenyi Biotech). Hereafter cells were stained for 20min at 4°C with the fluorochome-conjugated monoclonal antibodies described in **supplementary Table 2** and measured by flow cytometry. cDC2s were identified based on the expression of HLA-DR, CD1c, CD11c and FcεR1 (**Supplementary Figure 4A**).

Antigen processing and uptake by cDC2s

To study processing by cDC2s, PBMCs were thawed as previously described and directly incubated in complete medium with 0.5 µg/mL of DQ-green bovine serum albumin (BSA; Biovision) for 10 min at 37°C. Next, cells were washed, resuspended in complete medium and chased for 10, 30, 60 and 120 min. At the specific time points, samples were placed on ice and when all time points were collected, cells were washed twice with cold phosphate-buffered saline (PBS) (Sigma) with 0.1% FCS and 0.05% NaN3 (Immunosource), stained on ice for 15 min with the antibodies described in **supplementary Table 2** and measured by flow cytometry (**Supplementary Figure 4A**). BSA

processing by cDC2s was calculated as the median fluorescence intensity (MFI) of DQ-BSA normalized to T=0.

For BSA uptake assay, PBMCs were incubated in complete medium with 0.5µg/mL of BSA conjugated with Alexa Fluor 647 (Invitrogen) at 37°C. In addition, HC-PBMCs were primed with 1000U/mL of IFNα2a (Cell Sciences) or left in complete medium for 3h before BSA exposure. BSA uptake was monitored at 10, 30, 60 and 120 minutes. At the specific time point, samples were placed on ice and after all time points were collected, cells were washed twice with cold PBS (Sigma) with 0.1% FCS and 0.05% NaN3 (Immunosource), stained on ice for 15 min with the antibodies described in **supplementary Table 2** and measured by flow cytometry (**Supplementary Figure 4A**). BSA uptake was calculated as the median fluorescence intensity (MFI) of BSA-AF647 on cDC2s.

Interferon signature assessment

To determine the type I IFN-score, PBMCs were lysed in RLTPlus buffer (Qiagen) and total RNA was purified using AllPrep DNA/RNA/miRNA Universal Kit (Qiagen) according to the manufacturer's instructions. cDNA was synthesized using Superscript IV kit and quantitative-PCRs were performed on the QuantStudio 12k flex system (both Thermo Fisher Scientific). The expression of each IFN-induced genes (*IFI44L*, *IFI44*, *IFIT3*, *LY6E*, and *MX1*) was normalized to that of the endogenous *GAPDH* (**Supplementary Table 3**). The average IFN-score was calculated as previously described [8].

Uptake of apoptotic salivary gland epithelial cells by cDC2s

The human submandibular salivary gland (HSG) epithelial cell line (HTB-41) was kindly provided by Dr. Lynne Bingle (School of Clinical Dentistry, University of Sheffield). HSG cells were cultured in McCoy's 5A media (Thermo Fisher Scientific) supplemented with 1% penicillin/streptomycin (Thermo Fisher Scientific) and 10% FCS (Sigma-Aldrich).

HSG cells were stained with 0.1 µM of carboxyfluorescein succinimidyl ester (CFSE) (Thermo Fisher Scientific) and induced to apoptosis during 24h with 1 µM of staurosporine (Merck Chemicals BV), as previously described [9]. After that, supernatant was collected to preserve floating cells and adherent cells were rinsed with PBS (Sigma-Aldrich) and harvested by standard trypsinization. The

frequency of apoptotic HSG cells was assessed by annexin V staining according to the manufacturer's protocol. Cryopreserved PBMCs were thawed, rested and then either primed with or without IFNα2a, as previouly described, or co-cultured at a 1:1 ratio with apoptotic HSG cell suspension for 2h at 37°C. Cells were washed twice with cold PBS (Sigma) with 0.1% FCS and 0.05% NaN3 (Immunosource), stained on ice for 15 min with the antibodies described in **supplementary Table 2** and measured by flow cytometry (**Supplementary Figure 7**). Uptake of apoptotic HSG cells was quantified using the CFSE median fluorescence intensity (MFI).

cDC2s and CD4$^+$ T cell allogenic co-cultures

CD4$^+$ T cells were isolated from buffy coats (Sanquin) of 3 different donors by MACS using CD4$^+$ T Cell Isolation Kit (Miltenyi Biotec) according to the manufacturer's protocol. To ensure consistent purity and comparable T cell compartments of the isolated CD4$^+$ T cell, cells were stained with the antibodies described in **supplementary Table 2**. The purity of the isolated CD4$^+$ T cells was consistently above 90% for all the donors (**Supplementary Figure 8A**). cDC2s were isolated as described before and co-cultured in complete medium with allogenic CD4$^+$ T cells at a 1:5 ratio (cDC2s: T cells) for 3 days. To assess the proliferation rate of CD4$^+$ T cells, cells were labelled with 1.5 μM of CellTrace Violet (CTV) dye (Invitrogen), prior to co-culture. After 3 days of co-culture, cells were stained at 4°C for 10 min with fixable viability dye eFluor780 (eBioscience) to allow exclusion of dead cells, washed and stained at 4°C for 15 min with the antibodies described in **supplementary Table 2** and measured by flow cytometry (**Supplementary Figure 8B**). The percentage of proliferating CD4$^+$ T cells was measured as the proportion of CTV negative cells, and the expression of chemokine receptors on the cell-surface was evaluated within the proliferating CD4$^+$ T cells.

Flow cytometry data acquisition of all experiments was performed using a BD LSR Fortessa (BD Biosciences) and data were analyzed using FlowJo software (Tree Star).

Cytokine analysis

TNFα (Diaclone) and IFNγ (Thermo Fisher Scientific) levels were measured in cell-free supernatant of cDC2s-CD4$^+$ T cell co-culture using enzyme-linked immunosorbent assay following the manufacturer's instructions.

Phospho-Epitope Staining for Flow Cytometry

Peripheral blood mononuclear cells (PBMCs) were isolated and directly stained (T=0) or cultured at 1 × 10^6 cells/mL in complete medium. Cells were left unstimulated or were stimulated with toll-like receptor (TLR)4 ligand [Lipopolysaccharide (Invivogen)] for 15, 30 and 60 minutes. Next, PBMC were washed with phosphate-buffered saline (PBS) and fixed with 2% paraformaldehyde for 15 minutes at room temperature. After washing with cold PBS, cells were resuspended in cold PBS before drop wise addition of ice-cold methanol (ratio PBS: methanol; 1:9) and incubated on ice for 30min. Next, cells were washed with FACS Buffer and stained for 30min on ice with the antibodies described in **supplementary Table 2**. Data acquisition was performed using a BD LSR Fortessa (BD Biosciences) and data were analysed using FlowJo software (Tree Star). cDC2s were identified based on the expression of HLA-DR, CD1c, CD11c and FcεR1 (**Supplementary Figure 4A**).

Statistical Analysis

For RNA sequencing analysis, the Wald's test was used to identify DEGs in each pair-wise comparison performed between HC, nSS and pSS and the likelihood ratio test to identify DEGs considering multiple groups. Differences between the groups were analyzed by non-parametric test Mann-Whitney U-test and Kruskal-Wallis test, when appropriate. For the uptake and processing experiments at multiple time points the multiple comparison 2way ANOVA test with FDR correction was used. For the uptake experiments after IFNα priming at a single time point the paired t test was used. Statistical analyses and data visualization were performed using Python and R language, Graphpad Prism (GraphPad Software), MetaboAnalyst 4.0 [10] and ClustVis software [11]. Differences were considered to be statistically significant at $p < 0.05$.

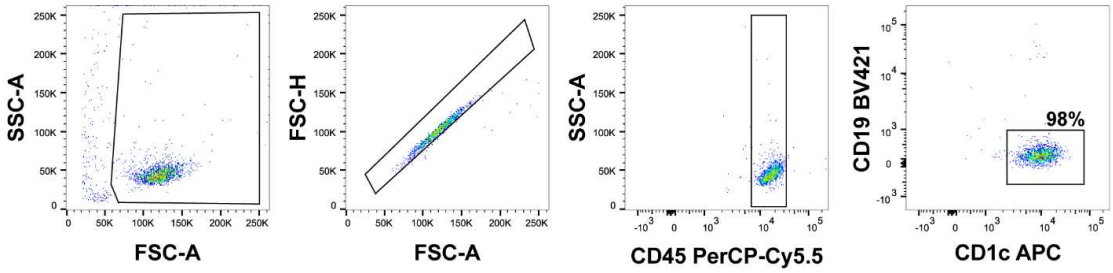

Supplementary Figure 1. Analysis strategy used to assess cDC2s purity. Flow cytometry gating strategy analysis to assess cDC2s purity after MACS isolation.

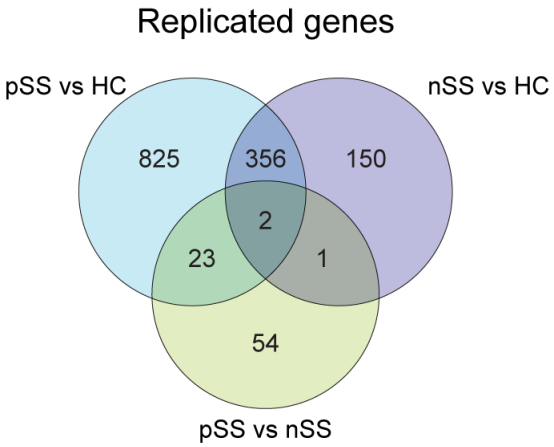

Supplementary Figure 2. Overlap of the replicated differentially expressed genes between pSS, nSS and HC. RNA sequencing of circulating cDC2s was performed independently for both discovery and replication cohort. Differentially expressed genes (DEGs) with a nominal p-value <0.05, average base mean expression >100 and with the same directionality in both cohorts were considered to be replicated. Venn diagrams show the overlap of the replicated differentially expressed genes (DEGs).

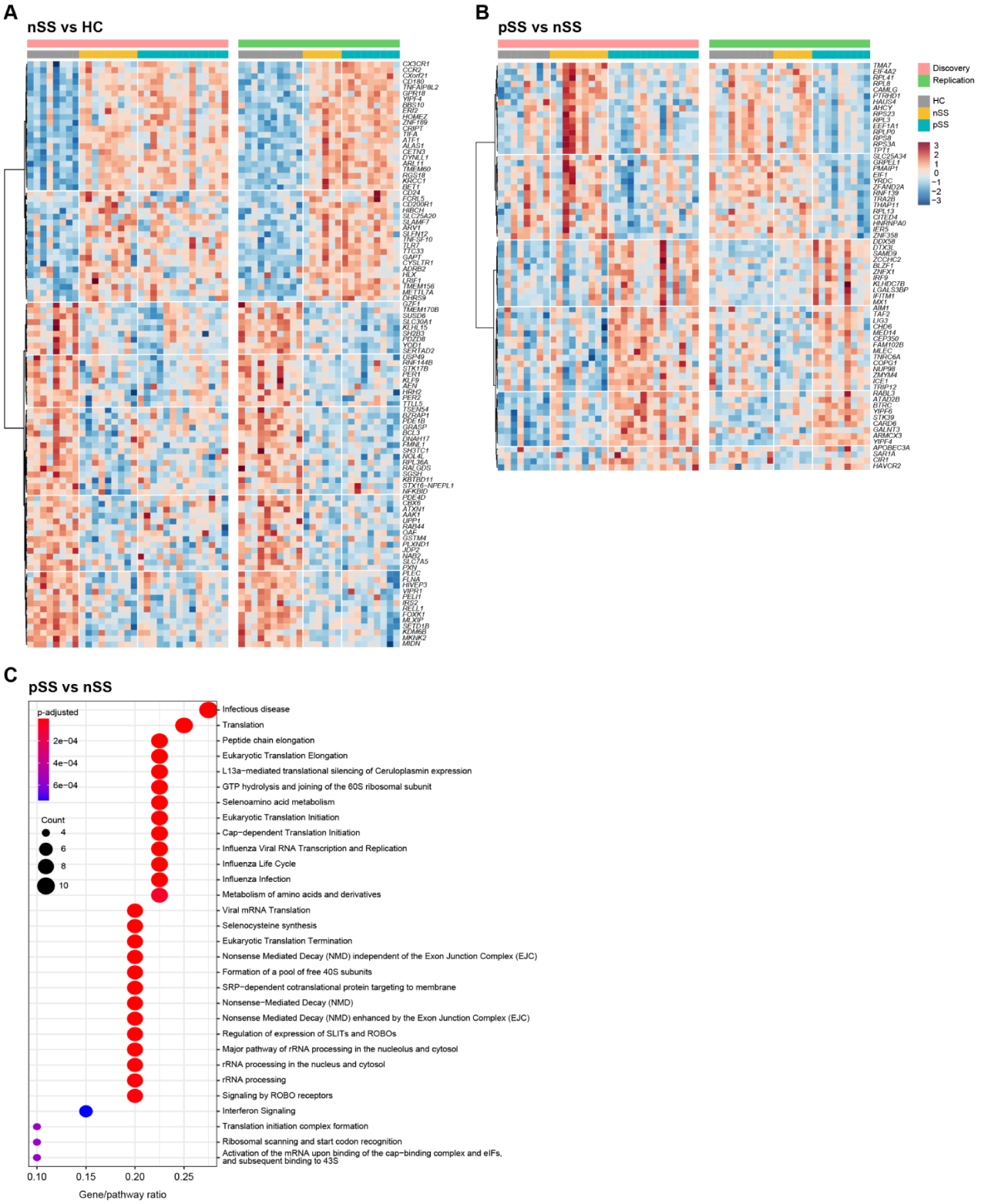
A
nSS vs HC
B
pSS vs nSS
Discovery
Replication
HC
nSS
pSS
C
pSS vs nSS
p-adjusted
2e−04
4e−04
6e−04
Count
4
6
8
10
Infectious disease
Translation
Peptide chain elongation
Eukaryotic Translation Elongation
L13a−mediated translational silencing of Ceruloplasmin expression
GTP hydrolysis and joining of the 60S ribosomal subunit
Selenoamino acid metabolism
Eukaryotic Translation Initiation
Cap−dependent Translation Initiation
Influenza Viral RNA Transcription and Replication
Influenza Life Cycle
Influenza Infection
Metabolism of amino acids and derivatives
Viral mRNA Translation
Selenocysteine synthesis
Eukaryotic Translation Termination
Nonsense Mediated Decay (NMD) independent of the Exon Junction Complex (EJC)
Formation of a pool of free 40S subunits
SRP−dependent cotranslational protein targeting to membrane
Nonsense−Mediated Decay (NMD)
Nonsense Mediated Decay (NMD) enhanced by the Exon Junction Complex (EJC)
Regulation of expression of SLITs and ROBOs
Major pathway of rRNA processing in the nucleolus and cytosol
rRNA processing in the nucleus and cytosol
rRNA processing
Signaling by ROBO receptors
Interferon Signaling
Translation initiation complex formation
Ribosomal scanning and start codon recognition
Activation of the mRNA upon binding of the cap−binding complex and eIFs, and subsequent binding to 43S
0.10
0.15
0.20
0.25
Gene/pathway ratio

Supplementary Figure 3. Transcriptomic characterization of circulating cDC2s from nSS patients. RNA sequencing of circulating cDC2s was performed independently for both cohorts. Heatmap shows the top 100 protein coding differentially expressed genes (DEGs) in both cohorts between nSS vs. HC in both cohorts (A). Heatmap of protein coding DEGs with a nominal p-value < 0.05 between pSS vs. nSS in both cohorts (B). Pathway enrichment analysis of the DEGs between pSS vs. nSS depicted in Supplementary Figure 3B. Columns show the number of DEGs found within the pathway over the total number of pathway components (ratio), dot-size depicts the number of genes used for enrichment analysis and color indicates the statistical significance (C).

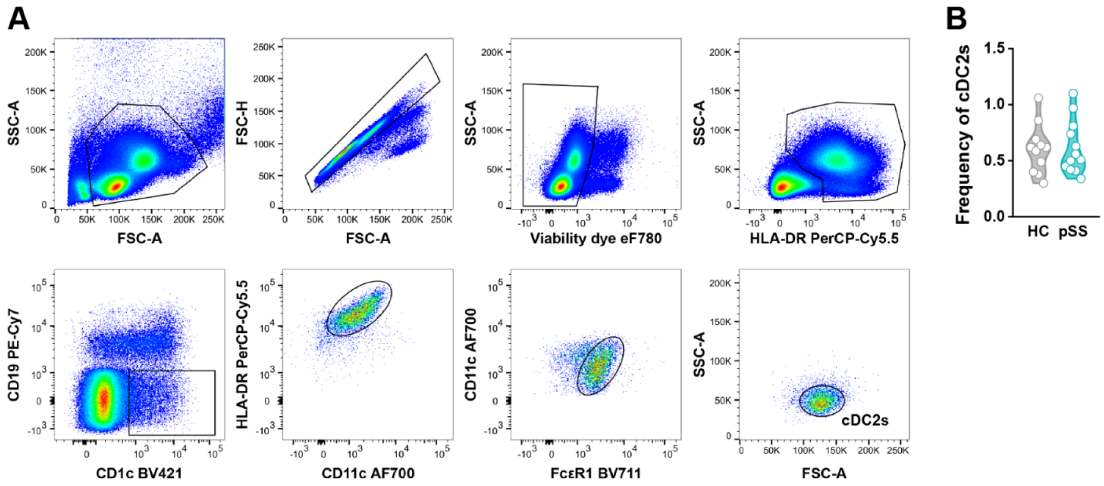

Supplementary Figure 4. Analysis strategy used to identify cDC2s in PBMCs. Representative flow cytometry gating strategy analysis to identify cDC2s in peripheral blood mononuclear cells (A). Violin plots depicts the frequency of circulating cDC2 in HC (n=11) and pSS patients (n=13) determined by flow cytometry (B).

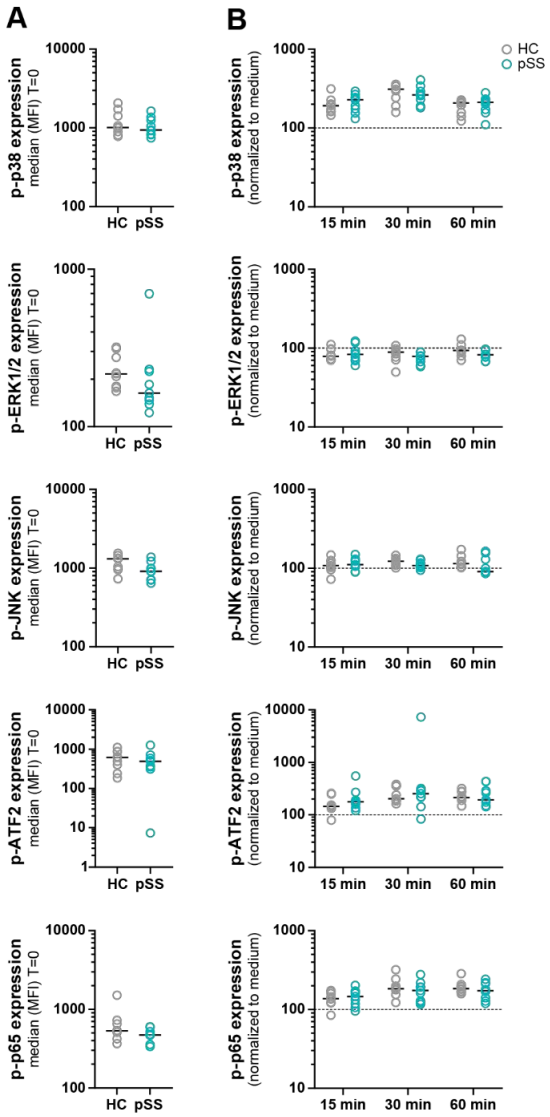

Supplementary Figure 5. Phosphorylation profile of cDC2s upon TLR4 activation. Phosphorylation levels of P38, ERK1/2, JNK, ATF2 and NF-kB were analyzed by flow cytometry in cDC2s of HC (n=9) and pSS patients (n=9) *ex-vivo* (basal level; T=0) (B) and after TLR4 stimulation at different time points. Phosphorylation results at the different time points was normalized to the respective medium condition (C).

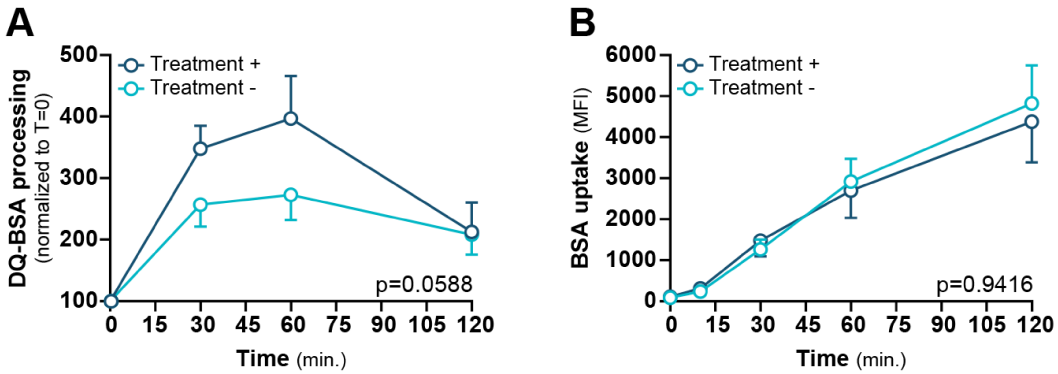

Supplementary Figure 6. Influence of pSS treatment on antigen processing and uptake by cDC2s. Peripheral blood mononuclear cells (PBMCs) were incubated with DQ–BSA for 10 minutes and the antigen processing by cDC2s was followed at the indicated time points. DQ-BSA processing represented as median fluorescence intensity (MFI) normalized to T=0, in treated pSS patients (Treatment +; n=7) and non-treated pSS patients (Treatment -; n=6) at different time points assessed by flow cytometry (A). Isolated PBMCs were incubated with AF647–BSA for the indicated time points and the uptake by cDC2s was assessed by flow cytometry. BSA uptake in treated pSS patients (Treatment +; n=8) and non-treated pSS patients (Treatment -; n=6) at different time points assessed by flow cytometry (B).

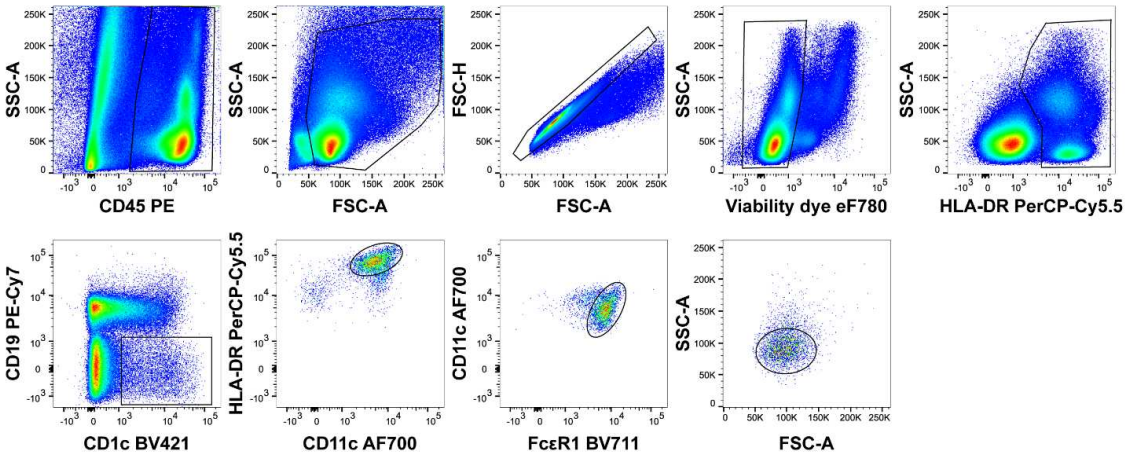

Supplementary Figure 7. Analysis strategy used to identify cDC2s in co-culture with apoptotic salivary gland (HSG)-epithelial cells. Representative flow cytometry gating strategy analysis to identify cDC2s in peripheral blood mononuclear cells after co-culture with apoptotic salivary gland (HSG)-epithelial cells.

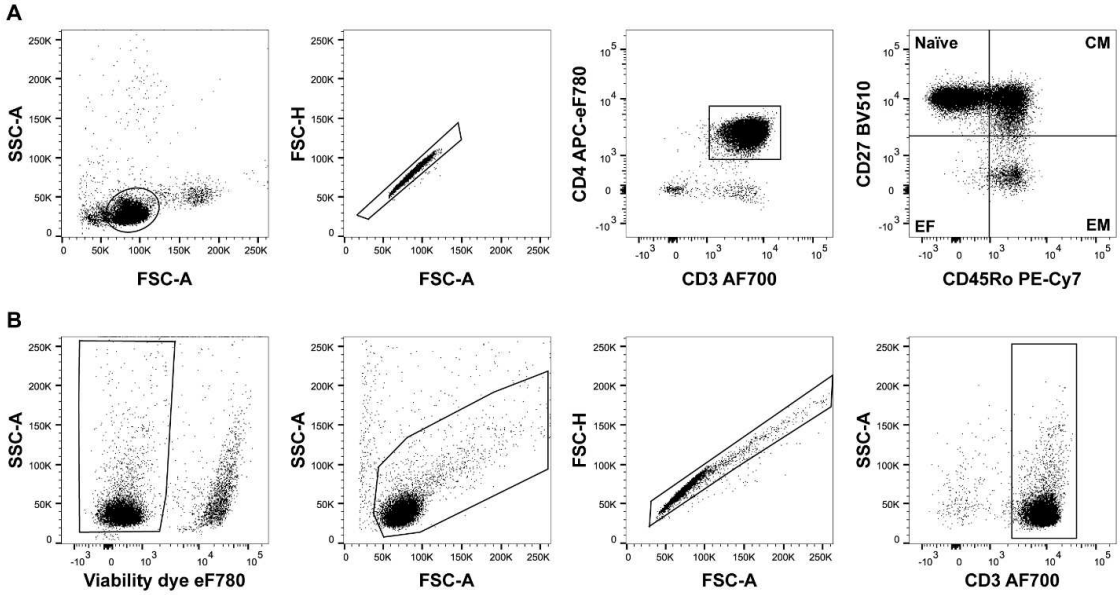

Supplementary Figure 8. Analysis strategy used to identify CD4$^+$ T cells subsets after MACS isolation and after co-culture with cDC2s. Representative flow cytometry gating strategy analysis of the different CD4$^+$ T cell subsets: naïve (CD27$^+$CD45Ro$^-$); CM: central memory (CD27$^+$CD45Ro$^+$); EM: effector memory (CD27$^-$CD45Ro$^+$); EF: effector (CD27$^-$CD45Ro$^-$) (A). Representative flow cytometry gating strategy analysis to identify CD3$^+$ T cells in cDC2s co-cultures (B).

Supplementary Table 1. Characteristics of the patients and controls enrolled in the validation experiments.

	Protein validation		**BSA uptake and processing**		**cDC2 – CD4⁺ T cell co-culture**	
	(n=44)		**(n=29)**		**(n=6)**	
	HC	pSS	HC	pSS	HC	pSS
N (M/F)	22 [1/21]	22 [1/21]	13 [0/13]	16 [0/16]	3 [0/3]	3 [0/3]
Age (yr.)	56 [25-78]	56 [21-76]	58 [35-63]	58 [41-78]	55 [43-60]	60 [56-65]
LFS (foci/4 mm^2)	-	3.0 [1.0-7.0]	-	1.7 [1.0-7.0]	-	1.4 [1.1-1.6]
ESSDAI	-	5.5 [1.0-15]	-	8.0 [0.0-16]	-	7.0 [0.0-7.0]
ESSPRI	-	7.0 [1.0-8.0]	-	7.0 [3.0-8.0]	-	6.0 [4.0-7.0]
Schirmer (mm/5 min)	-	3.0 [0.0-28]	-	1.5 [0.0-26]	-	12 [0.0-24]
ANA (no. positive [%])	-	18 [86%]	-	12 [75%]	-	2 [67%]
SSA (no. positive [%])	-	18 [82%]	-	12 [75%]	-	2 [67%]
SSB (no. positive [%])	-	13 [59%]	-	10 [63%]	-	1 [33%]
RF (no. positive [%])	-	12 [71%]	-	7 [78%]	-	2 [100%]
Serum IgG (g/L)	-	14 [7.0-33]	-	15 [8.4-26]	-	15 [9.0-16]
ESR (mm/hour)	-	15 [2.0-54]	-	18 [3.0-75]	-	10 [5.0-28]
C3 (g/L)	-	1.1 [0.8-1.6]	-	1.1 [0.9-1.4]	-	1.3 [1.2-1.4]
C4 (g/L)	-	0.2 [0.0-0.4]	-	0.2 [0.2-0.4]	-	0.3 [0.2-0.3]
Not treated (no. [%])	-	13 [59%]	-	8 [50%]	-	3 [100%]
Only HCQ (no. [%])	-	2 [9%]	-	3 [19%]	-	-
Other (no. [%])	-	7 [32%]	-	5 [31%]	-	-

HC: healthy control; pSS: primary Sjögren's syndrome; LFS: lymphocyte focus score; ESSDAI: EULAR Sjögren's syndrome disease activity index; ESSPRI: EULAR Sjögren's syndrome patient reported index; ANA: anti-nuclear antibodies; SSA: anti-SSA/Ro; SSB: anti-SSB/La; RF: rheumatoid factor; ESR: erythrocyte sedimentation rate; CRP: C-reactive protein, HCQ: hydroxychloroquine. Other treatment group includes for protein validation: azathioprine, alone (n=2) or in combination with prednisone (n=1); prednisone in combination with HCQ (n=2); methotrexate (n=2). For BSA uptake and processing: azathioprine (n=1), methotrexate, alone (n=1) or in combination with

hydroxychloroquine (n=1), hydroxychloroquine in combination with leflunomide (n=1) and hydroxychloroquine in combination with azathioprine and prednisone (n=1). Values are median [range] unless stated otherwise.

Supplementary Table 2. List of antibodies used for the flow cytometry stainings

Target	Label	Manufacturer	Clone	cDC2s Purity	Protein validation	Phospho flow	BSA uptake	DQ-BSA processing	CD4⁺ T cell purity	cDC2s-CD4⁺ T cell
BDCA1	APC	eBioscience	L161	x						
CD14	FITC	Miltenyi	TÜK4	x						
CD19	BV421	Biolegend	HIB19	x						
CD20	PE	eBioscience	2H7	x						
CD45	PerCP	Biolegend	HI30	x						
FceR1	BV711	Biolegend	AER-37		x					
CX3CR1	FITC	Biolegend	2A9-1		x					
BAFF	PE	Biolegend	T7-241		x					
CD18 (ITGB2)	FITC	Biolegend	TS1/18		x					
IFNAR1	PE	Thermo Scientific	85228		x					
PLXND1	FITC	FAB4160G			x					
PLXNB2	APC	FAB53291A			x					
HLA-DR	PerCP-Cy5.5	Biolegend	L243		x	x	x	x		
CD11c	AF700	eBioscience	3.9		x			x		
CD14	APC-eF780	eBioscience	61D3		x		x	x		
CD19	PE-Cy7	Beckman Coulter	J3-119		x		x	x		
BDCA1	BV421	Biolegend	L161		x		x	x		
BDCA1	AF488	Sony Biotechnology	L161			x				
CD14	APC-H7	BD Biosciences	MϕP9			x				
CD11c	PE-CF594	BD Biosciences	B-ly6			x				
CD19	BV711	Biolegend	HIB19			x				
Phospho-p38	AF647	Cell signaling Techn	28B10			x				
Phospho-ATF2	PE	Anbnova	G3			x				
P-p44/42 (ERK1/2)	PB	Cell signaling Techn	197G2			x				
P-NF-kB p65	AF647	BD Biosciences	K10-895			x				
Phospho-JNK	PE	BD Biosciences	N9-66			x				
CD16	V500	BD Biosciences	3G8				x	x		
FceR1	FITC	eBioscience	AER-37				x			
CD11c	PE	BD Biosciences	B-LY6				x			
FcεR1	PE	eBioscience	AER-37					x		
CD8	PerCP-Cy5.5	Biolegend	RPA-T8						x	
CD4	APC-eF780	eBioscience	RPA-T4						x	
CD56	PE-CF594	BD Biosciences	B159						x	
CD27	BV510	BD Biosciences	L128						x	
CXCR3	FITC	Biolegend	G025H7							x
CXCR5	PerCP-Cy5.5	Biolegend	J252D4							x
CD27	APC	BD Biosciences	L128							x
CD3	AF700	Biolegend	UCHT1						x	x
Viability dye	eF780	eBioscience	n.a.							x
CCR4	PE	BD Biosciences	1G1							x
CD45Ro	PE-Cy7	BD Biosciences	UCHL1						x	x

Supplementary Table 3. Sequences of primers used for RT-qPCR

Gene	Primer forward 5′ – 3′	Primer reverse 5′ – 3′
IFI44L	CCACCGTCAGTATTTGGAATGT	ATTTCTGTGCTCTCTGGCTT
IFI44	TTTGCTCTTTCTGACATCTCGGT	TCCTCCCTTAGATTCCCTATTTGC
IFIT3	ACTGTTTCAACGGGTGTTGG	CCTTGTAGCAGCACCCAATC
LY6E	ATCTGTACTGCCTGAAGCCG	GTCACGAGATTCCCAATGCC
MX1	GCATCCCACCCTCTATTACTG	CGCACCTTCTCCTCATACTG
GAPDH	GCCAGCCGAGCCACATC	TGACCAGGCGCCCAATAC

SUPPLEMENTARY REFERENCES

1. Hillen MR, Pandit A, Blokland SLM, et al. Plasmacytoid DCs From Patients With Sjogren's Syndrome Are Transcriptionally Primed for Enhanced Pro-inflammatory Cytokine Production. *Front Immunol*. 2019;10:2096.

2. Yates A, Akanni W, Amode MR, et al. Ensembl 2016. *Nucleic Acids Res*. 2016;44(D1):D710-6.

3. Dobin A, Davis CA, Schlesinger F, et al. STAR: ultrafast universal RNA-seq aligner. *Bioinformatics*. 2013;29(1):15-21.

4. Anders S, Pyl PT, Huber W. HTSeq--a Python framework to work with high-throughput sequencing data. *Bioinformatics*. 2015;31(2):166-9.

5. Risso D, Ngai J, Speed TP, et al. Normalization of RNA-seq data using factor analysis of control genes or samples. *Nat Biotechnol*. 2014;32(9):896-902.

6. Love MI, Huber W, Anders S. Moderated estimation of fold change and dispersion for RNA-seq data with DESeq2. *Genome Biol*. 2014;15(12):550.

7. Yu G, He QY. ReactomePA: an R/Bioconductor package for reactome pathway analysis and visualization. *Mol Biosyst*. 2016;12(2):477-9.

8. Brkic Z, Maria NI, van Helden-Meeuwsen CG, et al. Prevalence of interferon type I signature in CD14 monocytes of patients with Sjogren's syndrome and association with disease activity and BAFF gene expression. *Ann Rheum Dis*. 2013;72(5):728-35.

9. Hauk V, Fraccaroli L, Grasso E, et al. Monocytes from Sjogren's syndrome patients display increased vasoactive intestinal peptide receptor 2 expression and impaired apoptotic cell phagocytosis. *Clin Exp Immunol*. 2014;177(3):662-70.

10. Chong J, Wishart DS, Xia J. Using MetaboAnalyst 4.0 for Comprehensive and Integrative Metabolomics Data Analysis. *Curr Protoc Bioinformatics*. 2019;68(1):e86.

11. Metsalu T, Vilo J. ClustVis: a web tool for visualizing clustering of multivariate data using Principal Component Analysis and heatmap. *Nucleic Acids Res*. 2015;43(W1):W566-70.